EUV and Soft X-ray Quantum Efficiency Measurements of a Thinned, Back-Illuminated CMOS Active Pixel Sensor

Robert A. Stern, Lawrence Shing (Lockheed Martin Solar and Astrophysics Laboratory)
Nick Waltham (Rutherford Appleton Laboratory)
Andrew Harris, and Peter Pool (e2v)

ABSTRACT

We report first absolute effective quantum efficiency (e-h pairs collected/predicted) measurements of a monolithic, thinned, back-illuminated CMOS Active Pixel Sensor (APS) in the EUV and soft X-ray region (13-600 Å). The sensor was designed and fabricated under a joint RAL/e2v research program, and characterized in the Lockheed Martin Solar and Astrophysics (LMSAL) XUV calibration facility. We compare our QE results to data and models developed for thinned CCDs with similar back surface passivation. Our results demonstrate that CMOS APS arrays show significant promise for use in space-based solar physics and astrophysics missions.

INTRODUCTION

CMOS APS devices are rapidly emerging as potential replacements for scientific CCDs in space-based solar and astrophysical instruments. Despite significant advantages in radiation hardness, reduced power consumption, and individual pixel addressability, however, the current generation of CMOS arrays are not yet to sufficiently mature to replace scientific CCDs. This is especially true for applications requiring soft X-ray or EUV sensitivity, hence back illumination. In this poster, we report the first measurements of a monolithic, back-illuminated, ion-implanted, laser annealed CMOS array in the XUV region.

CMOS APS CHARACTERISTICS

The device undergoing testing at LMSAL is one of six CMOS APS designs contained on a test structure developed by Rutherford Appleton Laboratory (RAL) and e2v. This device (labeled "Ben" in Figure 1) consists of a 512x512 array of 10 μm square 3T pixels. The entire test structure was fabricated on 14 μm epitaxial material, and back-thinned for use at EUV wavelengths. A detailed description of the test structure and characterization of each of the designs at visible wavelengths is described in detail by Waltham et al. (2007).

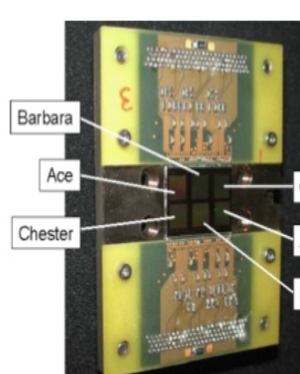

Figure 1. CMOS APS Test Structure

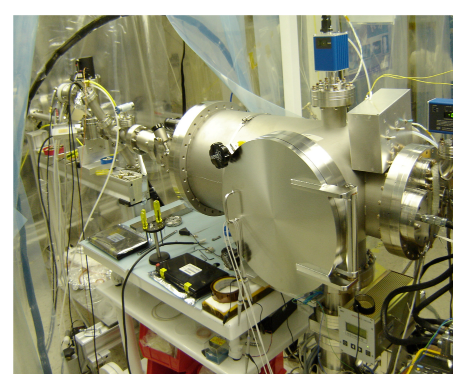

Figure 2. LMSAL Test Chamber

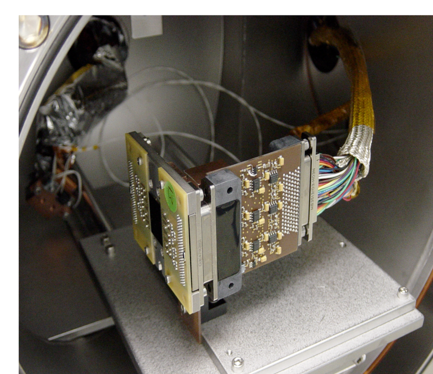

Figure 3. APS Test Structure Mounted in Chamber

BASIC DEVICE PERFORMANCE

At LMSAL, we first performed a series of visible light tests on "Ben" to verify the basic device performance characteristics. All measurements were made at -86 C in a dedicated low-contamination high vacuum chamber originally developed for characterizing CCDs for the Solar Dynamics Observatory (Figs. 2 & 3). All measurements were made with an ARC Gen III Camera with IR array processor running at an effective readout rate of 1 Mpix/sec. Photon transfers and visible light flat fields indicated a noise performance slightly higher (~33 e RMS) than reported (~ 25 e) in Waltham et al. (2007; see Figure 4). A flat-field image taken in visible light is shown in Figure 5, with any large-scale features from a non-uniform light source removed via subtracting a 4th order quadratic polynomial and scaled such that the color table represents a range of +/- 10%. The most notable features in the image are the result of an overlapping laser anneal treatment applied to passivate the back surface. This pattern is very similar to that seen in e2v CCDs with comparable back surface treatments (see, e.g., Stern et al 2004).

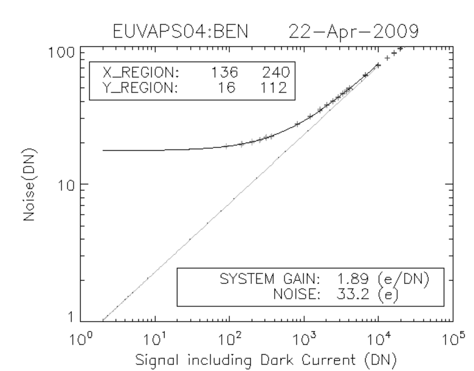

Figure 4. Photon Transfer Curve

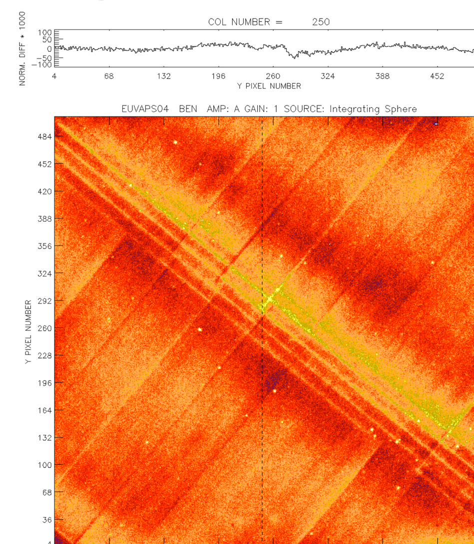

Figure 5. Visible Flat Field (see text)

^{55}FE MEASUREMENTS

After visible light characterization, we exposed the APS to an ^{55}Fe source (5.9 and 6.4 keV photons) to verify system gain and noise performance. Thirty ^{55}Fe frames were taken to increase counting statistics and obtain an accurate X-ray histogram. An example of a single frame of ^{55}Fe single photon events in shown in Figure 6. The system noise dominated over Fano type noise; nevertheless, by selecting single events, we were able to discern both the Kα and Kβ peaks, and estimate an energy resolution of ~ 330 eV FWHM (Figure 7), roughly 3 times that expected from a Fano-noise limited device at this energy. The charge spreading was mostly limited to a ~3x3 pixel region surrounding the peak pixel for the X-ray events. Although not "state-of-the-art" compared to single photon-counting X-ray CCDs, the device performance is quite sufficient to proceed to quantum efficiency measurements.

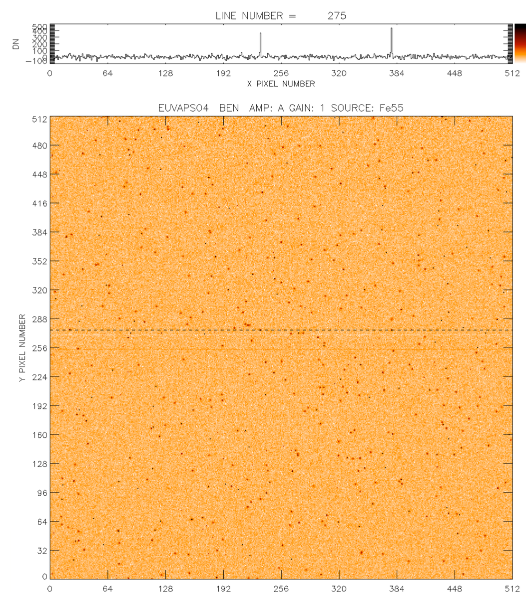

Figure 6. ^{55}Fe Image. Horizontal dashed line indicates row sampled with line plot above image.

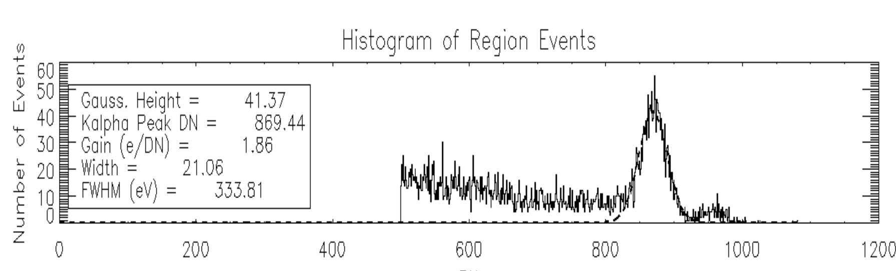

Figure 7. ^{55}Fe single-photon histogram (single events only). Events taken from total of 30 separate images. Note fitted system gain is consistent with that from photon transfer curve obtained in visible light (Fig. 4)

XUV MEASUREMENTS

All device quantum efficiency measurements were performed in the LMSAL XUV Calibration Facility, which was also used for similar absolute QE measurements of the GOES 13 & 14 SXI CCDs (Stern et al. 2004), and the SDO AIA CCDs (to be published). The system consists of: a 1 m grazing incidence monochromator with X-ray and XUV sources; a beam collimator chamber; a "reflectometer" chamber, which is used to position either a gas proportional counter or microchannel plate detector used for beam calibration; and a detector chamber (see Figure 8). At the detector location, the beam size is roughly a few mm, with dimensions determined by the source and various slits in the system (ahead of the calibration detector). Since the entire beam fits on both the calibration detector and the device to be measured (see below), the "effective QE" in equivalent photons detected/input photons (see Stern, Shing, and Blouke 1994) can be measured by knowing the calibration detector absolute response (accurate to ~ 5% for the PPC; ~ 10% for the MCP referenced to a NIST-calibrated EUV photodiode); the CMOS detector (inverse) gain in e/DN (previously determined); and assuming the canonical 3.62 eV/e-h pair for X-ray and XUV photons.

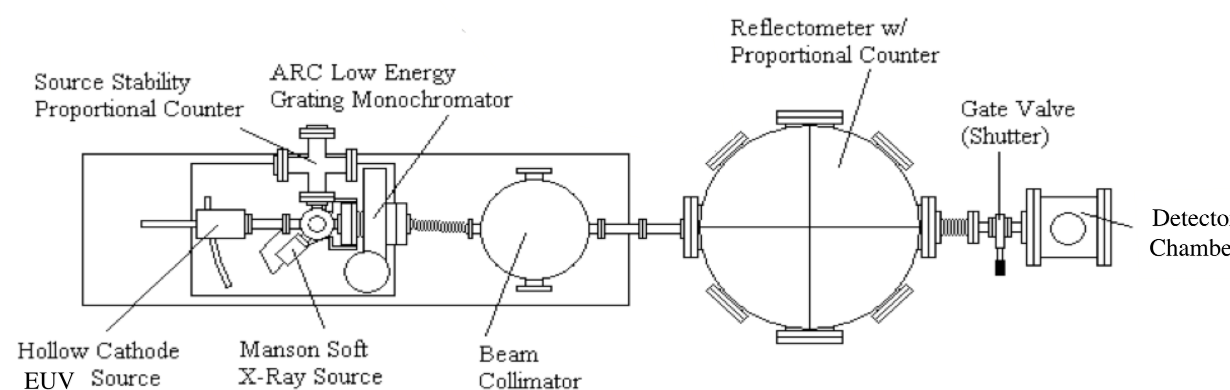

Figure 8. Schematic of LMSAL XUV Calibration System.

QE COMPARISONS AND MODELING

In Figure 10 we show the effective QE results measured for "Ben" compared with a thinned CCD with a similar backside treatment developed by e2v for the STEREO/SECCHI program. We derived models for both devices' response using a variation of the "empirical" model discussed in Stern, Shing, and Blouke (1994): in particular, we allowed the charge collection efficiency (CCE) of each device to be scaled by a constant factor (see Table 1 for derived model parameters). This was necessary to produce an acceptable fit for the "Ben" CMOS device. Even so, some of the derived parameters for "Ben" (see orange entries in Table 1) suggest that our model does not completely account for the behavior of the CMOS device compared to the SECCHI CCD. Known losses within the CMOS pixel structure probably account for much of the non-unity CCE; however, the derived oxide layer thickness (primarily required by the lower than expected 304 Å response) is also too large for a typical native oxide (25-40 Å) on back-thinned silicon.

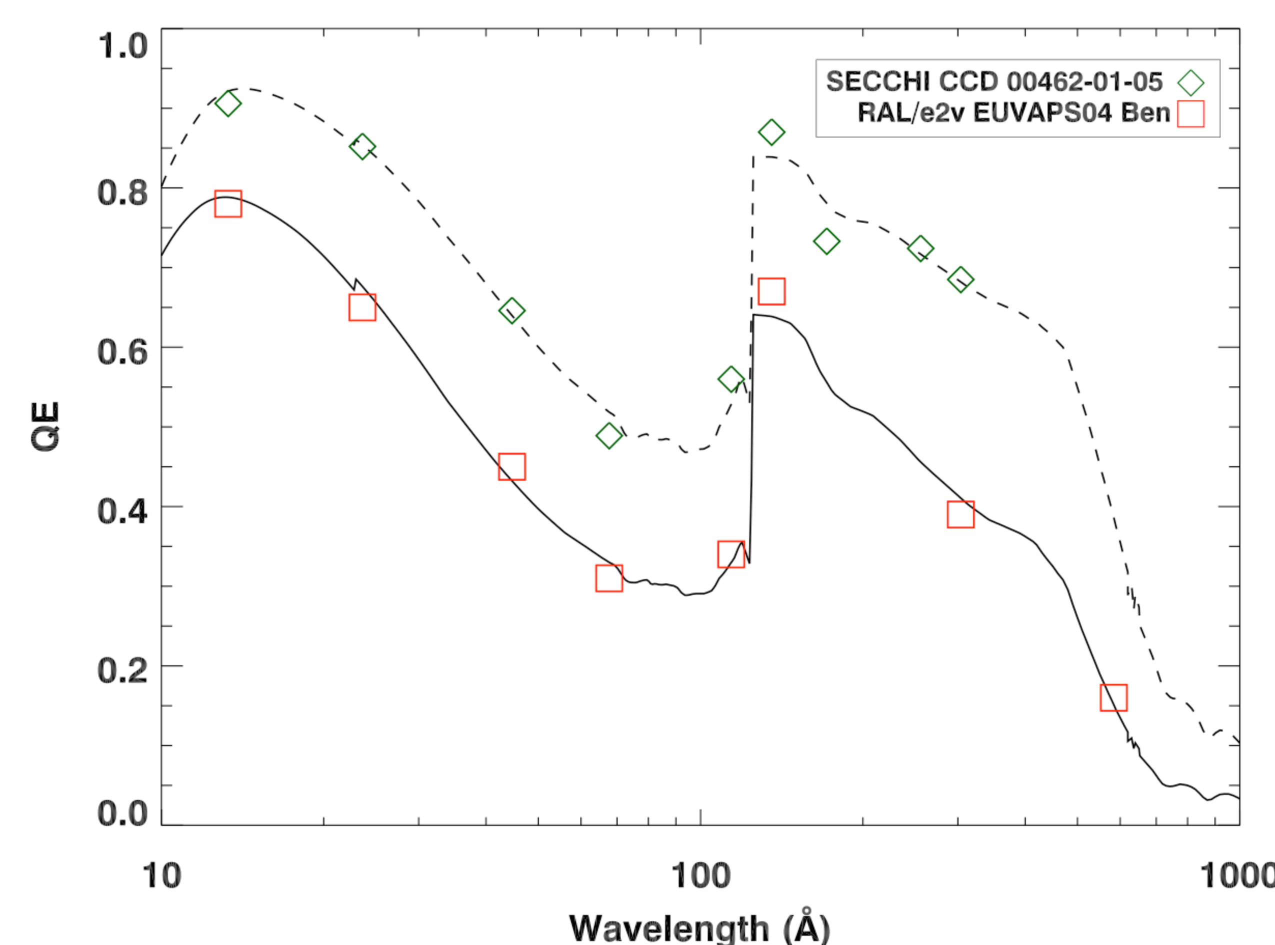

Figure 10. Effective quantum efficiency (equivalent photons detected/incident photons) for "Ben" CMOS APS device (red squares) and model (solid line: see discussion in text and fitted model parameters in Table 1 below). For comparison, measurements for a back-thinned CCD processed in a similar fashion for the STEREO/SECCHI instrument are shown (data: green diamonds; model: dashed line).

Device	Secchi CCD	EUVAPS "Ben"
"CCE < 1" region (Å)	2184	3495
Min CCE	0.41	0.32
Substrate Depth (μm)	8.8	9.6
Surface Oxide (Å)	34.	83.
CCE Scaling Factor	0.97	0.85

Table 1. Derived model parameters from fits shown in Fig. 10 for the SECCHI CCD and "Ben" CMOS APS device. Model formulation is that used in Stern, Shing, and Blouke 1994 for ion-implanted, laser-annealed CCDs, with the addition of a charge collection efficiency (CCE) scaling or normalization factor. Results for the CMOS APS device suggest that some device characteristics require additional modeling.

REFERENCES

Stern, R.A., et al., 2004, Proc. SPIE 5171, 77.
Stern, R.A., Shing, L., and Blouke, M., 1994, Appl. Opt., 33, 2521.
Waltham, N. et al. , 2007, Proc. SPIE 6690, 669007.

RESULTS

We obtained images at seven soft X-ray and EUV wavelengths (23, 45, 68, 114, 170, 304, and 584 Å). Typical exposures were 200 sec, and each image was dark subtracted using a dark image taken at the same exposure time and temperature. Example images are shown in Figure 9a-c for 45, 68, and 304 Å. The variations in beam shape are from changes in light source and slit dimensions: for each wavelength the position of the CMOS array and calibration reference detector positions were adjusted to ensure that the entire beam (within a few %) fell on both detectors.

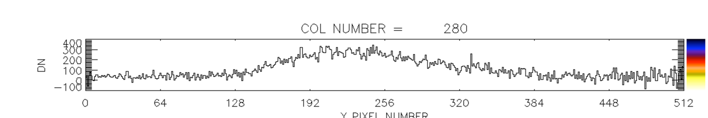

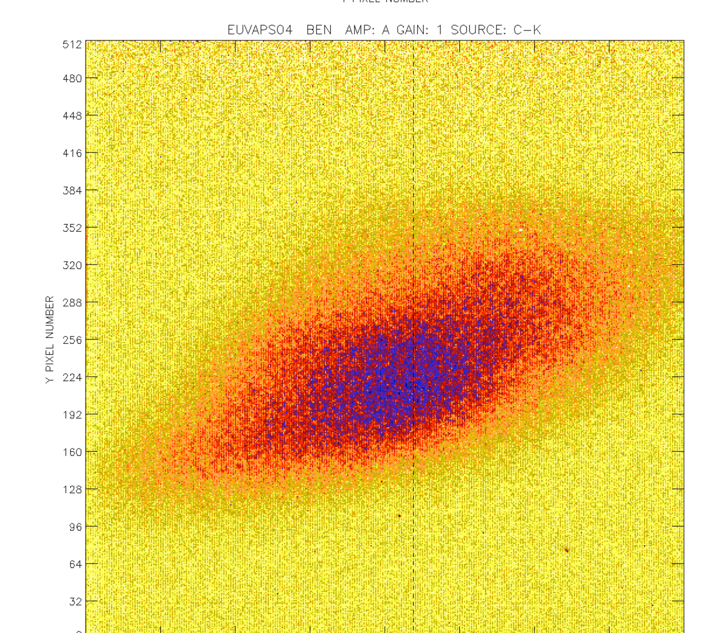

Figure 9 (a). Carbon K (45 Å) image taken with "Ben" CMOS APS device. Integration time is 200 s. A dark exposure of the same length has been subtracted from the image. The vertical dashed line indicates the column (280) which was used to make the line plot shown above the image.

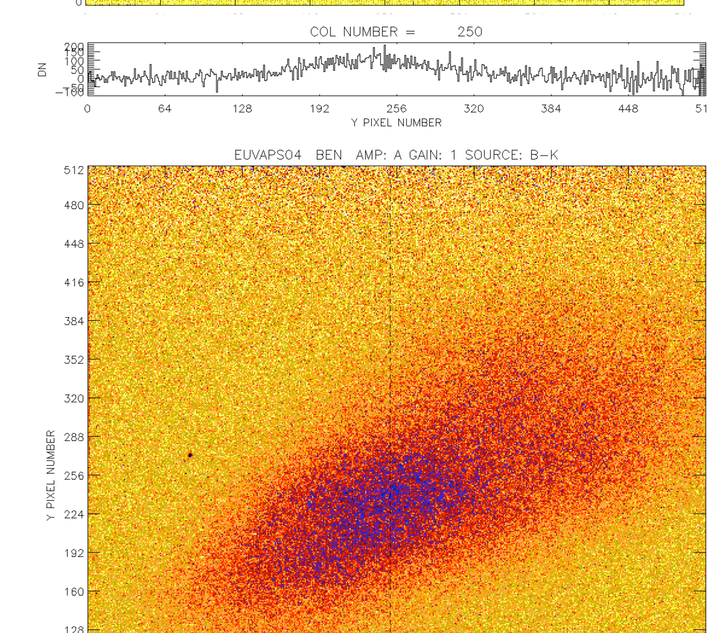

Figure 9 (b). Boron K (68 Å) image taken with "Ben" CMOS APS device.

Figure 9 (c). He II (304 Å) image taken with "Ben" CMOS APS device. Note difference in beam shape compared to Figs 9a and b resulting from use of hollow cathode discharge source.

SUMMARY

We have measured the effective QE of a thinned, back-illuminated CMOS APS in the EUV/soft X-ray range. To our knowledge, these are the first measurements of an ion-implanted, laser-annealed CMOS sensor in this wavelength region. Our results are encouraging in that the absolute QE values are similar to, though slightly lower than, comparable measurements of CCDs produced using a similar back-thinning process, and are quite practical for use in future spaceborne solar physics or astrophysics missions.